

## Characterizing 6 August 2007 Crandall Canyon mine collapse from ALOS PALSAR InSAR

ZHONG LU\*<sup>†</sup> and CHARLES WICKS, Jr.<sup>‡</sup>

<sup>†</sup>US Geological Survey, Vancouver, WA, USA

<sup>‡</sup>US Geological Survey, Menlo Park, CA, USA

(Received 10 December 2009; in final form 15 January 2010)

We used ALOS InSAR images to study land surface deformation over the Crandall Canyon mine in Utah, which collapsed on 6 August 2007 and killed six miners. The collapse was registered as a  $M_L$  3.9 seismic event. An InSAR image spanning the time of the collapse shows 25–30 cm surface subsidence over the mine. We used distributed dislocation sources to model the deformation field, and found that a collapse source model alone does not adequately fit the deformation field. Normal faulting is also required, such that the event is best characterized as a ‘trapdoor’ collapse. The calculated moment of the normal fault is about the same as the moment of the collapse source, with each larger than the seismically computed moment. Our InSAR results, including the location of the event, the extent of the collapsed area, and constraints on the shearing component of the deformation source, all confirm and extend recent seismic studies of the 6 August 2007 event.

### 1. Introduction

A portion of the Crandall Canyon mine, located in central Utah (figure 1) collapsed on 6 August 2007, killing six miners (e.g. Pechmann *et al.* 2008). A subsequent collapse 10 days later killed three rescuers and injured six others. These collapses were registered as local magnitude ( $M_L$ ) 3.9 and 1.6 seismic events having locations and origin times coincident with the collapses.

The epicentre of the 6 August 2007  $M_L = 3.9$  seismic event (figure 2) was first determined by the regional seismic network. Standard methods for earthquake location determination utilize seismic wave arrival times to triangulate the source of the seismic waves while first motions of the P wave or waveform inversions are used to compute the style of faulting. The location errors depend primarily on the accuracy of the seismic velocity model, the accuracy of analyst picks of phase arrivals, and the geometric distribution of seismic stations. Due to the relatively large spacing of seismic stations near the Crandall Canyon mine at the time of the 6 August 2007 event, the estimated 1-standard deviation uncertainty of the epicentre is about 0.4 km (<http://earthquake.usgs.gov/eqcenter/eqinthenews/2007/uu00007535/>). The initial event location is about 1.5 km WSW of the collapsed mine (figure 2). The nearest seismic station is about 19 km from the event. Consequently, there is an even

---

\*Corresponding author. Email: [lu@usgs.gov](mailto:lu@usgs.gov)

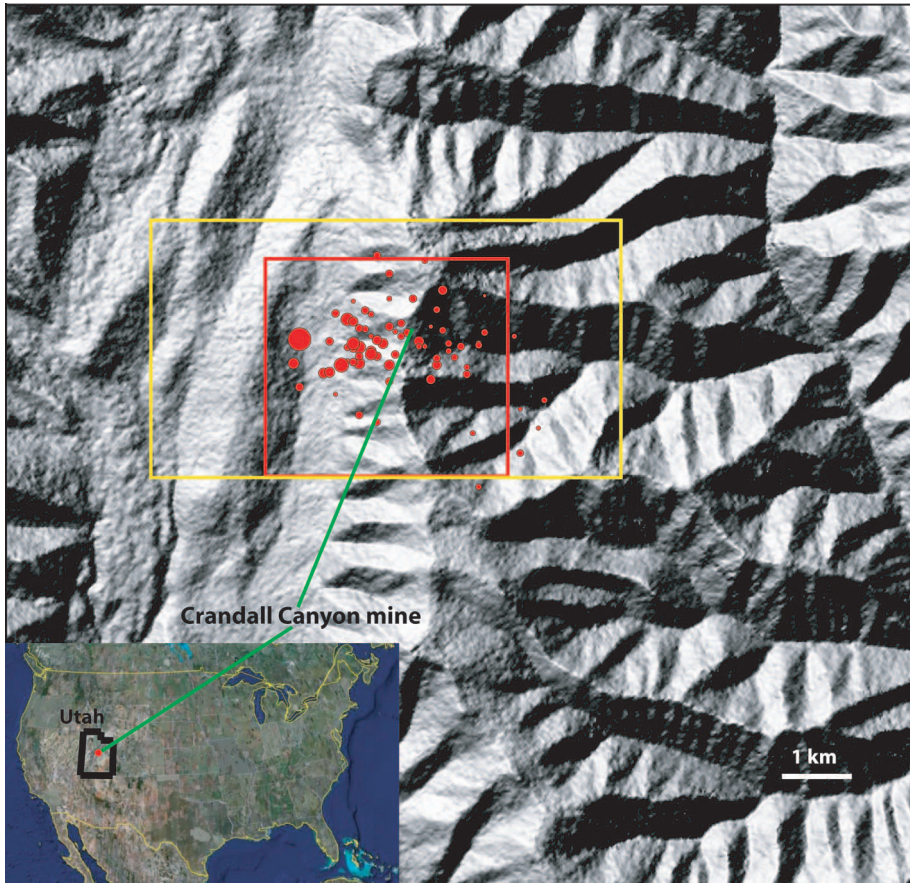


Figure 1. Map of mining-induced seismicity (with  $M_L > 1.6$ ) over the Crandall Canyon mine area during January and October 2007. The red and yellow polygons represent the coverage of interferograms in figures 2 and 3, respectively. The inset map showing the location of Crandall Canyon mine is produced using Google Earth.

larger uncertainty in the initial depth estimate of the source. The initially reported depth is  $1.6 \pm 1.0$  km. The 6 August 2007 event was relocated by repacking the P-wave arrival times, using stations within 100 km of the epicentre only, as well as choosing a localized velocity model (figure 2). The relocation furnished on 16 August 2007 (<http://www.seis.utah.edu/MONRESEARCH/CM/locations.htm>) put the epicentre about 1 km south the collapsed mine (figure 2).

A temporary network of five stations was deployed near the Crandall Canyon mine starting 8 August 2008 in order to better locate aftershocks associated with the collapse. The combined regional and temporary network recorded the second mine collapse on 17 August 2007 and determined that the  $M_L = 1.6$  seismic event occurred at 0.3 km depth. Using the 17 August 2007 earthquake as a master event (e.g. Wechsler and Smith 1978, Waldhauser and Ellsworth, 2000), Pechmann *et al.* (2008) carefully relocated the 6 August 2007 seismic event. The relative relocation procedures provided a more accurate location of the initial collapse based on constraints from a more accurately located aftershock. The derived epicentre of the 6 August 2007 event is less than 300 m from the collapsed portion of the mine.

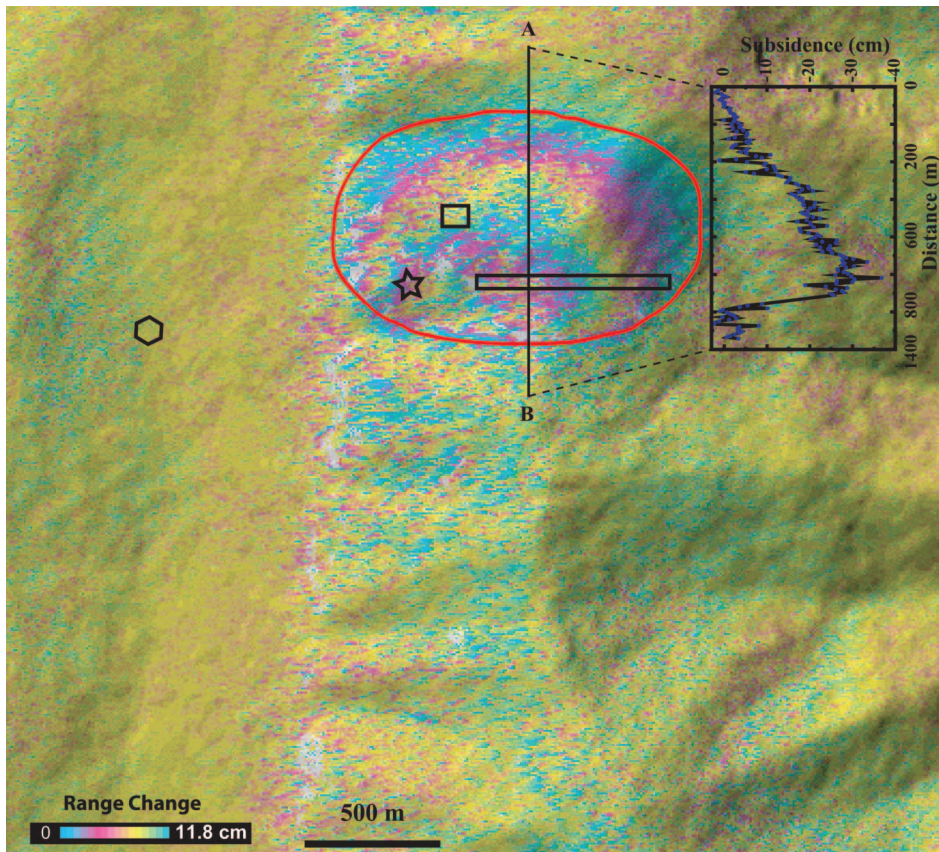


Figure 2. InSAR image spanning 8 June 2007 to 8 September 2007 and epicentres of the 6 August 2007 seismic events that were determined by four different methods. The hexagon represents the initial epicentre from the standard relocation programme. The circle represents the epicentre using a localized velocity structure. The square represents the epicentre from the master-event method. The star represents the epicentre from the double-difference relocation method. The damaged area of the Crandall Canyon mine estimated by the MSHA (Pechmann *et al.* 2008) is shown as the elongated narrow rectangle. InSAR phase observations are draped over a shaded relief image. One fringe represents a range change of 11.8 cm along the satellite look direction. Areas of loss of InSAR coherence are not coloured. Also shown is the vertical displacement along a profile A–B, showing a peak value of about 30 cm.

In this paper, we present an analysis of interferometric synthetic aperture radar (InSAR) images over the Crandall Canyon mine area. InSAR has been used to study both natural earthquakes (e.g. Massonnet *et al.* 1993) and nuclear explosions (e.g. Vincent *et al.* 2003), as well as mining-induced subsidence (e.g. Ge *et al.* 2007). We show that InSAR deformation data unambiguously determine the location of the 6 August 2007 event and provide further insights into the nature of the mine collapse.

## 2. InSAR observation and analysis

We obtained both C-band (wavelength of 5.66 cm) Envisat synthetic aperture radar (SAR) images and L-band (wavelength of 23.6 cm) Advanced Land Observing

Satellite (ALOS) Phased Array type L-band SAR (PALSAR) images over the Crandall Canyon mine region. Due to relatively dense vegetation in the study area, C-band InSAR images did not maintain coherence over a 35-day-revisit time period. Therefore, we focused our efforts on analysing available L-band InSAR images from the Japan ALOS PALSAR sensor. Six PALSAR images were acquired over the Crandall Canyon mine in 2006 and 2007, which we used to produce 4 InSAR images (figures 2 and 3). Topographic phase contributions in the original interferograms were removed by using the 1-arc-second Shuttle Radar Topography Mission (SRTM) digital elevation model (DEM).

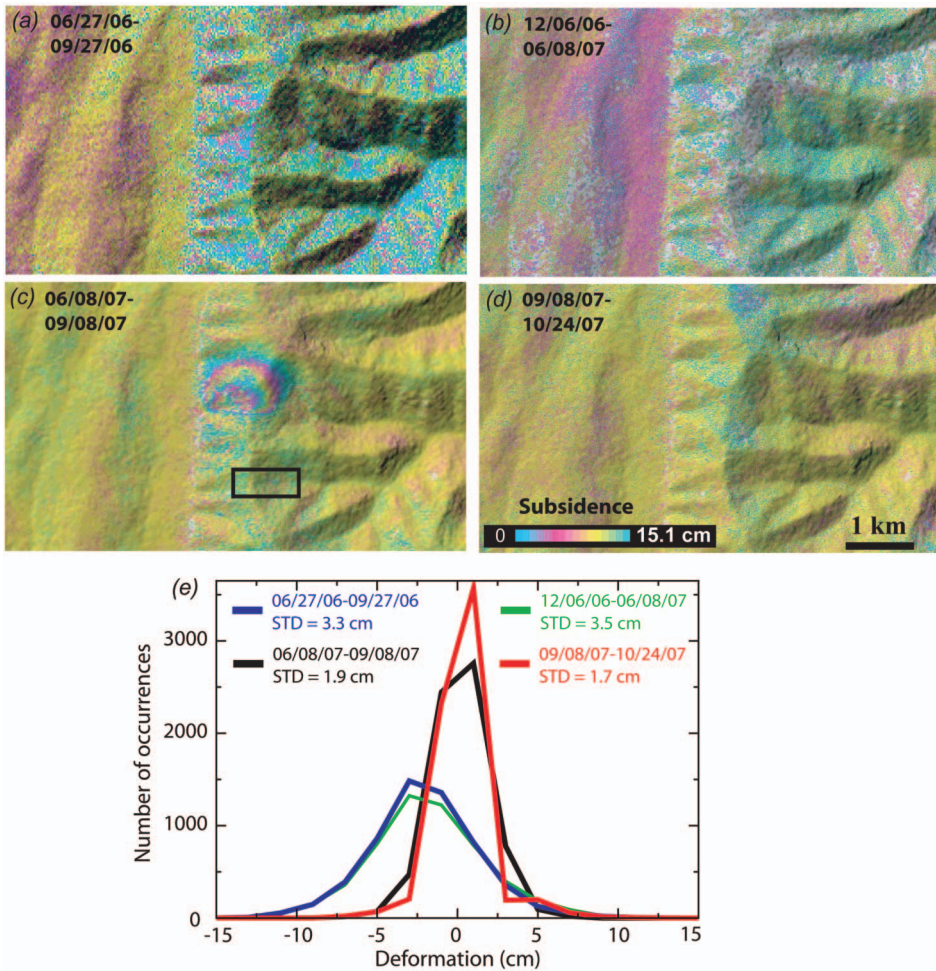


Figure 3. InSAR images over Crandall Canyon mine that span the following time intervals: (a) 27 June 2006 and 27 September 2006, (b) 6 December 2006 and 8 June 2007, (c) 8 June 2007 and 8 September 2007, and (d) 8 September 2007 and 24 October 2007. InSAR phase observations are draped over a shaded relief image. (e) Histograms and uncertainties of InSAR phase values in the rectangle (c) for all four interferograms in figures (a)–(d). The InSAR phase value was converted to vertical surface displacement. One fringe represents a range change of 11.8 cm along the satellite look direction, which is equivalent to 15.1 cm vertical displacement. Areas of loss of InSAR coherence are not coloured.

Figure 2 shows the June–September 2007 image that brackets the 6 August 2007 event. No deformation can be found over the 6 August 2007 event epicentre determined by the standard relocation method (figure 2). Instead, we observe an ellipse-shaped region that encloses the damaged area estimated by Department of Labor’s Mine Safety and Health Administration (MSHA) and the epicentres derived from the master-event method and the double difference relocation technique by Pechmann *et al.* (2008). The major axis of the ellipse is about 1.5 km and the minor axis about 1 km. The surface displacement field is not symmetric, with most displacement occurring over the southern one-third portion of the ellipse.

The interferogram shown in figure 2 is an ascending InSAR image, with a look angle of about  $38.7^\circ$  from the vertical. This means that the interferogram is slightly more sensitive to vertical motion than horizontal motion. The phase changes in the interferogram suggest range increases over the centre of the deformed area. Assuming the displacement is vertical, a range increase of 11.8 cm (i.e. 1 fringe) corresponds to about 15.1 cm subsidence. We plot the subsidence along a profile A–B (figure 2). The peak subsidence is  $\sim 30$  cm. However, subsidence is not symmetrical; instead, it is concentrated dominantly in the southern end, with a sharp break in phase gradient along the southern edge of the ellipse.

The extent of the deformation detected by InSAR (figure 2) suggests that the collapse area is likely to extend farther west of the MSHA’s 600 m by 80 m collapse-area estimate (Pechmann *et al.* 2008). The InSAR observation is also consistent with the improved epicentre and the inference that the collapse started near the western end. The seismic moment estimate by Ford *et al.* (2008) suggested the area of the collapse should be about twice as large as the collapse area estimated by the MSHA, which is consistent with our result.

In figure 3 we show a few InSAR images to illustrate the deformation before, during, and after the 6 August 2007 collapse. We also plot histograms of these interferograms over a small area that possesses a similar coherence property to the area of collapsed mine, to illustrate the uncertainties of the observed deformation in all four interferograms. The interferograms spanning 27 June 2006 to 27 September 2006 (figure 3(a)) and 6 December 2006 to 8 June 2007 (figure 3(b)) are noisier than the other two interferograms (figures 3(c) and (d)) due either to relatively larger baselines or longer time separations. Based on standard deviations of deformation measurements in the two interferograms (figure 3(e)), we may not be able to detect any deformation of less than 7 cm at the 95% confidence level. In other words, the deformation, if any, would likely be less than about 7 cm over 3- to 6-month time periods between June 2006 to June 2007 (figure 3(a) and (b)). The 8 September 2007 to 24 October 2007 InSAR image (figures 3(d)) had the best coherence, with a standard deviation of 1.7 cm in vertical deformation (figure 3(e)). During that time interval, no deformation of larger than 3 cm (at 95% confidence level) can be observed over the Crandall Canyon mine. Therefore, we conclude that most of the subsidence observed in the 8 June 2007 – 8 September 2007 InSAR image (figure 2) was likely due to the mine collapse on 6 August 2007.

### 3. Deformation modelling and discussion

The sharp break in phase gradient on the south edge of the deformation signal in the interferogram (figure 2) is an important observation that indicates the source is more complicated than a simple collapse source. To model the interferograms, we first

used the quad-tree algorithm to resample the InSAR data by reducing the large number of highly correlated data points in the InSAR image (e.g. Jónsson *et al.* 2002, Simons *et al.* 2002). We then investigated the data with a model that consists of a distributed set of dislocations (Okada 1985) within a homogenous elastic half-space. The dislocation, or ‘slip’, distribution is described functionally by a two-dimensional Weibull distribution (e.g. Myrhaug and Rue 1998). Note that we use the term slip to mean shear movement or surface perpendicular movement. The Weibull distribution is versatile in that it can take the shape of an exponential distribution, a Rayleigh distribution, an approximate Gaussian distribution or other types of distributions, depending on the shape parameter. We use it here as a smoothing function that allows the slip to taper to a near zero value at edges of the model. We add more versatility by allowing truncation in the amplitude and lateral extent of the slip distribution. This allows, respectively, an area of uniform slip within the slip distribution and a sharp discontinuity in slip in one direction. The use of a Weibull distribution assumes that the slip is continuous within the slip distribution. The functional form of slip distribution enables us to systematically explore model space with nonlinear least-squares techniques.

Initially, we model the deformation source solely as a distributed collapse source and find an adequate fit only where the depth of a flat lying source is less than  $\sim 100$  m. We define an adequate fit as a model for which the variance of the residual (observed data minus calculated) is reduced to the same variance as the noise in the non-deforming area of the interferogram. We know that the depth of drill holes used to locate trapped miners ranged from 430 m to 620 m (Pechmann *et al.* 2008, and references therein), which is consistent with the depth of longwall mining at Utah and the well-located aftershocks following the 6 August 2007 mine collapse. Therefore, our simple collapse model with spatially varying collapse volume is inconsistent with observational and seismological constraints. The depth from our model source is chiefly constrained by the steep phase gradient in the interferograms, which requires a component to the deformation source shallower than the known depth of the mine collapse.

To better model the deformation source we constrain the depth of a flat lying collapse source to be 500 m and add a shallow uniform-slip normal fault that dips to the north. We constrain the dip of the normal fault to fall between  $0^\circ$  and  $90^\circ$  and the depth to the top of the fault to be between 0 and 500 m. The best-fit model includes a normal fault that dips  $40^\circ$  to the north. Using an F-test we note that the dip of the normal fault is not well constrained; at an estimated 95% confidence level, the dip is between  $20^\circ$  and  $85^\circ$ . For all dips the top of the fault is shallow, shallower than 70 m and deeper than 20 m. The shearing component of our model is supported by the seismological analysis of Ford *et al.* (2008) and Dreger *et al.* (2008). These authors noted that purely vertical closing of a flat crack could not explain the large Love waves observed at some seismic stations and argued that an additional shear mechanism is needed to fully explain the observed waveforms. The normal fault in our model is not meant to represent a naturally occurring earthquake. More likely it represents responsive slip of the cantilevered strata along the mine’s longwall or other weak zones, which resulted in a trapdoor configuration for the collapse.

The ratio between the normal fault and the collapse component decreases from about 2.5 at  $20^\circ$  dip to  $\sim 0.3$  at a dip of  $85^\circ$ . In the seismic source characterization of Ford *et al.* (2008) the authors estimated the collapse mechanism for two different source decompositions to be 78 and 79% of the total moment. This requires the dip to be near 85 degrees if the moment ratio is the same for the geodetic source as it is for

the seismic source. The moment magnitude of the geodetic source with a dip for the normal fault component of  $85^\circ$  is 4.49, whereas Ford *et al.* (2008) found a moment magnitude of 4.12. The calculated geodetic moment increases with decreasing dip angle to about 4.58 at  $20^\circ$  dip. We prefer a steep dip for the normal fault component to minimize differences with the seismic source determined by Ford *et al.* (2008). We expect additional collapse and slip on the normal fault could lead to the larger geodetic moment, but these processes might also lead to a different moment ratio between the collapse and normal fault components. In figure 4, we show an example of the calculated best-fit model for a normal fault component dip of  $65^\circ$ . This model has a geodetic moment magnitude 4.5 and a low moment ratio ( $\sim 0.57$ ), but the fault also

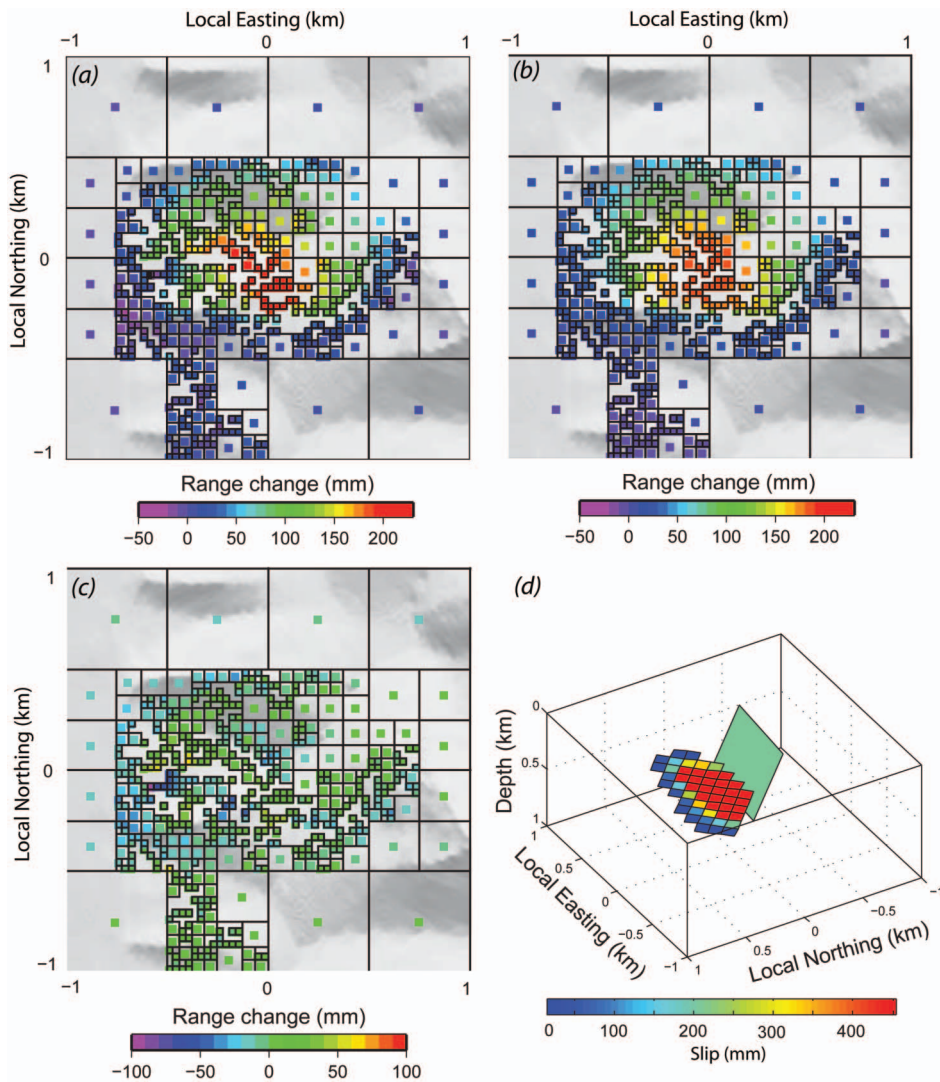


Figure 4. (a) Observed, (b) modelled and (c) residual deformation interferograms. The modelled InSAR image is based on the best-fit model parameter from distributed dislocations that includes a normal fault dipping at  $65^\circ$ . (d) Model geometry and slip distribution.

intersects the modelled collapse area, whereas a model with a dip of  $85^\circ$  for a normal fault is too steep to intersect the modelled collapse area.

The amount of collapse and the areal extent of the collapse in the model are variable. The peak collapse varies from about 0.3 m to 0.7 m while the areal extent of the modelled collapse varies from about 0.4 to 0.6 km<sup>2</sup>. Ford *et al.* (2008) estimated a collapse range of 0.06 to 0.55 m for the seismic source and a collapse area of 0.11 to 1 km<sup>2</sup>. They favoured the larger collapse values that would correspond with smaller areas of collapse. Pechmann *et al.* (2008) inferred a collapse area of  $\sim 0.2$  km<sup>2</sup> and an average collapse value of 0.3 m. There is good agreement between our study and the two seismic studies at least for the collapse component. Based on the evidence above, we suggest the extent of damaged area during the August 2007 mine collapse might be much larger than the MSHA estimate of 0.05 km<sup>2</sup> (Pechmann *et al.* 2008).

#### 4. Conclusion

InSAR deformation analysis clearly reveals the location of the 6 August 2007 event, which could not be precisely determined before the addition of a local seismic network and the assistance of a large aftershock event. The combination of InSAR observation as well as seismic data analysis from first motion directions (Pechmann *et al.* 2008) and moment tensor inversion (Ford *et al.* 2008) provides insights into the collapse of Crandall Canyon mine. The observed subsidence of about 30 cm is directly over the Crandall Canyon mine, suggesting that the 6 August 2007 seismic event occurred within or immediately above the mine. The pattern of the observed deformation (away-from-satellite range lengthening) also suggests the deformation is not caused by a natural occurring earthquake, which is consistent with the seismological observations and modelling of the event (Pechmann *et al.* 2008, Ford *et al.* 2008, Dreger *et al.* 2008).

A collapse source alone could not adequately fit the deformation field; a normal fault was also required. The dip of the normal fault is not well constrained, falling somewhere between  $20^\circ$  and  $85^\circ$ ; however, the location of the surface trace is robustly stable. The calculated moment of the normal fault is about the same as the moment of the collapse source with each larger than the seismic moment of the event.

We conclude that InSAR observation of the ground surface over the Crandall Canyon mine provides unique information about the mine collapse, which compliments seismic first-motion analysis and seismic moment tensor inversion of waveforms. InSAR results in this study (1) pin down the location of the 6 August 2007 seismic event that was the signature of the mine collapse, (2) suggest location errors of the seismic event from the standard epicentre relocation method, (3) determine an estimate of the extent of the collapsed area, and (4) provide new constraints on a shearing component of the mine collapse. Routine monitoring of land surface subsidence from satellite InSAR will provide constraining information about future mine collapses, especially over poorly instrumented areas.

#### Acknowledgements

PALSAR data are copyrighted JAXA/METI and were provided by Alaska Satellite Facility. We thank S. Moran, H. Benz, and D. Dzurisin for thorough reviews and detailed comments. We appreciate the useful discussions by J. Pechmann and M. Gauna.

## References

- DREGER, D., FORD, S. and WALTER, W., 2008, Source analysis of the Crandall Canyon, Utah, mine collapse. *Science*, **321**, p. 217.
- FORD, S.R., DREGER, D.S. and WALTER, W.R., 2008, Source characterization of the 6 August 2007 Crandall Canyon Mine seismic event in central Utah. *Seismological Research Letters*, **79**, 637–644.
- JÓNSSON, S., ZEBKER, H., SEGALL, P. and AMELUNG, F., 2002, Fault slip distribution of the 1999 Mw 7.1 Hector Mine, California, earthquake, estimated from satellite radar and GPS measurements. *Bulletin of the Seismological Society of America*, **92**, pp. 1377–1389.
- GE, L., CHANG, H.C. and RIZOS, C., 2007, Mine subsidence monitoring using multi-source satellite SAR images. *Photogrammetric Engineering & Remote Sensing*, **73**, pp. 259–266.
- MASSONNET, D., ROSSI, M., CARMONA, C., ADRAGNA, F., PELTZER, G., FEIGL, K. and RABAUTE, T., 1993, The displacement field of the Landers earthquake mapped by radar interferometry. *Nature*, **364**, pp. 138–142.
- MYRHAUG, D. and RUE, H., 1998, Joint distribution of successive wave periods revisited. *Journal of Ship Research*, **42**, pp. 199–206.
- OKADA, Y., 1985, Surface deformation due to shear and tensile faults in a half-space. *Bulletin of the Seismological Society of America*, **75**, pp. 1135–1154.
- PECHMANN, J., ARABASZ, W., PANKOW, K., BURLACU, R. and MCCARTER, M., 2008, Seismological Report on the 6 August 2007 Crandall Canyon Mine Collapse in Utah. *Seismological Research Letters*, **79**, pp. 620–636.
- SIMONS, M., FIALKO, Y. and RIVERA, L., 2002, Coseismic deformation from the 1999 Mw7: 1 Hector Mine, California, earthquake, as inferred from InSAR and GPS observations. *Bulletin of the Seismological Society of America*, **92**, pp. 1390–1402.
- VINCENT, P., LARSEN, S., GALLAWAY, G., LACZNIAK, R., FOXALL, B., WALTER, W. and ZUCCA, J., 2003, New signatures of underground nuclear tests revealed by satellite radar interferometry. *Geophysical Research Letters*, **30**, p. 2141.
- WALDHAUSER, F. and ELLSWORTH, W.L., 2000, A double-difference earthquake location algorithm: method and application to the Northern Hayward Fault, California. *Bulletin of the Seismological Society of America*, **90**, pp. 1353–1368.
- WECHSLER, D. and SMITH, B., 1978, An evaluation of hypocenter relocation techniques with applications to southern Utah: regional earthquake distributions and seismicity of the geothermal areas. Department of Energy publication DOE/ET/28392-32, DOI: 10.2172/6579471. Available online at: <http://www.osti.gov/energycitations> (accessed 16 February 2010).